

Abstract

Rock bridges in rock masses would increase the bearing capacity of Non-persistent discontinuities. In this paper the effect of ratio of rock bridge surface to joint surface, rock bridge shape and number of rock bridge on failure behaviour of intermittent rock joint were investigated. A total of 18 various models with dimensions of 15 cm × 15 cm × 15 cm of plaster specimens were fabricated simulating the open joints possessing rock bridge. The introduced rock bridges have various continuities in shear surface. The area of the rock bridge was 45 cm² and 90 cm² out of the total fixed area of 225 cm² respectively. The fabricated specimens were subjected to shear tests under normal loads of 1 MPa in order to investigate the shear mechanism of rock bridge. The results indicated that the failure pattern and the failure mechanism were affected by two parameters; i.e. the configuration of rock bridge and ratio of rock bridge surface to joint surface. So that increasing in joint in front of the rock bridge changes the shear failure mode to tensile failure mode.

Keywords

Rock bridges, joint, shear and tensile failure mode

1 Introduction

The length scale of fractures founds in natural rocks ranges from tens of kilometers down to tens of microns. In addition, fractures or joints in rocks are normally of finite length or are discontinuous in nature. In some rare cases, it is possible that the failure in the rock mass is limited to a single discontinuity. Generally, several discontinuities exist in various sizes, which constitute a combined shear surface. In this sense, the areas which are located between the neighbouring discontinuities are called the Rock Bridges (see the definition in Figure 1). The presences of rock bridges in not fully persistent natural discontinuity sets are a significant factor affecting the stability of rock structures and have the greatest importance for the shear resistance of the failure surface [1, 2].

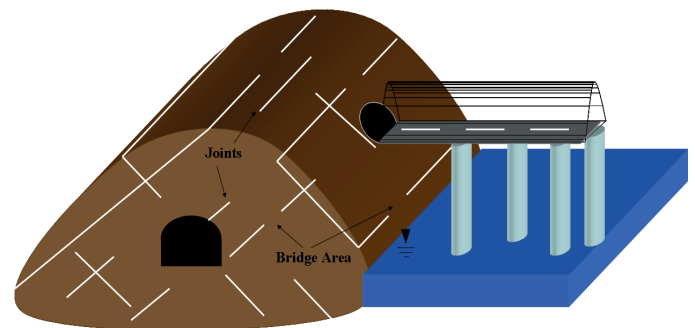


Fig. 1 Rock bridges in discontinuously-jointed rock.

One claims to be on the safe side since the rock bridges are thought to produce a strength reserve, as they have to be broken first before failure can take place along the newly separated plane. Also, the coalescence of non-persistent joint causes rock failure in slopes, foundations and tunnels. Therefore, a comprehensive study on the shear failure behaviour of jointed rock can provide a good understanding of both local and general rock instabilities, leading to an improved design for rock engineering projects. A number of experimental studies have been carried out to investigate the crack initiation, propagation and coalescence in the axial or biaxial test conditions (e.g. [3-5]). Two types of cracks can initiate from the tips of the two-dimensional pre-existing non-persistent discontinuity: (1) wing cracks; and

¹ Department of Mining Engineering, Hamedan University of Technology, Mardom street, P.O.B. 65155-579

² Institute for Rock Mechanics and Tunnelling, Technische Universität Graz, Rechbauerstraße 12, A-8010 Graz

* Corresponding author, email: vahab.sarfarazi@gmail.com

(2) secondary cracks; see Figure 2. Wing cracks, also called primary cracks, are tensile cracks that initiate at an angle from the tips of the flaw and propagate in a stable manner towards the direction of maximum compression. Secondary cracks are shear cracks that also initiate from the tips of the flaws and initially propagate in a stable manner.

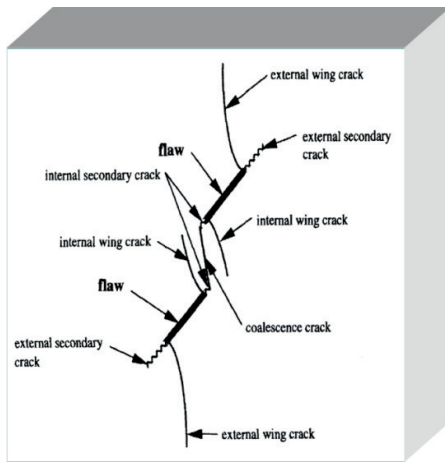


Fig. 2 Crack pattern in pre-cracked specimens of rock materials in uniaxial compression [5].

The pattern of coalescence between two parallel crack in both modelling materials and natural rocks have been done in direct shear boxes (e.g. [6, 7]). Lajtai [8] performed direct shear test on natural rock specimens with two parallel slots, tensile wing cracks were found to first appear at the tips of horizontal joints, followed by the secondary shear cracks propagating towards the opposite joint. Also he observed that the failure mode changed with increasing normal stress; he suggested a composite failure envelope to describe the transition from the tensile strength of the intact material to the residual strength of the discontinuities. He thus recognized that maximum shear strength develops only if the strength of the solid material and the joints are mobilized simultaneously. Savilahti et al. [9] did some further study on the specimens of jointed rock under direct shear tests where the joint separation varies in both horizontal and vertical directions and joint arrangement changes from non-overlapping to overlapping using modelling material. The coalescence patterns for the specimens indicated that the jointed rock failed in mixed mode for non-overlapping joint configuration and in tensile mode for overlapping joint form. Wong et al. [10] studied shear strength and failure pattern of rock-like models containing arrayed open joints in both modelling plaster material and natural rocks under direct shear tests. The results showed that failure pattern was mainly controlled by the joint separation while shear strength of jointed rock depended mostly on the failure pattern. Ghazvinian [11, 12] made a thorough analysis of the shear behaviour of the rock-bridge based on the change in the rock-bridge persistency. The analysis shows that the failure mode and the failure mechanism

are under the effect of the continuity of the rock-bridge. Also, a number of experimental studies have been carried out to investigate the crack initiation, propagation and coalescence in different loading condition (Yang et al., [13, 14]; Fujii and Ishijima, [15]; Wasantha et al., [16]; Zhang and Wong [17, 18], Bahaaddini et al. [19], Sarfarazi et al. [20]). Since this rock segments have different configuration in shear surface, therefore we come up with this question that weather the rock bridge configuration influences the shear properties along the shear surface. This article is an answer to this question. In fact, in this article the influence of number and configuration of rock bridges on shear properties have been analysed.

2 Experimental studies

The discussion of experimental studies is divided into four sections. The first section discusses the physical properties of a modelling material, the second section is describing the technique of preparing the jointed specimens, the third section is focused on the testing procedure and finally, the fourth section considers the general experimental observations and discussions.

2.1 Modeling material and its physical properties

The material used for this investigation is gypsum, the same material was used by Takeuchi [21], Shen et al. [22] and Bobet et al. [23]. Gypsum is chosen because, in addition to behave same as a weak rock, is an ideal model material which a wide range of brittle rocks can be represented; second, all the previous experiences and results can be incorporated and the earlier findings can be compared with the new ones; third, it allows to prepare a large number of specimens easily; Forth, repeatability of results. The samples are prepared from a mixture of the water and gypsum with a ratio of water to gypsum = 0.75. Concurrent with the preparation of specimens and their testing, uniaxial compression and indirect tensile strengths of the intact material was also tested in order to control the variability of material. The uniaxial compressive strength (UCS) of the model material is measured on fabricated cylindrical specimens with 56 mm in diameter and 112 mm in length. The indirect tensile strength of the material is determined by the Brazilian test using fabricated solid discs 56 mm in diameter and 28 mm in thickness. The testing procedure of uniaxial compressive strength test and the Brazilian test complies with the ASTM D2938-86 [24] and ASTM C496-71 [25], codes respectively. The base material properties derived from unconfined compression and tensile test are as follows:

Average uniaxial compressive strength:	14 MPa
Average brazilian tensile strength:	1.2 MPa
Average Young's Modulus in compression:	3600 MPa
Average Poisson's ratio:	0.18

2.2 The technique in preparing the jointed specimens

The procedure developed by Bobet [9] for preparing open non-persistent joints was used in this research with some modifications. The material mixture is prepared by mixing water and gypsum in a blender; the mixture is then poured into a steel mold with internal dimension of $15 \times 15 \times 15$ cm. The mold consists of four steel sheets bolted together and of two PMMA plates, 1/6 inch thick, which are placed at the top and bottom of the mold. As shown in Figure 3 the top plate has two rectangular openings used to fill the mold with the liquid gypsum mixture. The upper and the lower surfaces have slits cut into them. The width of slits is 0.5 mm (0.02 inch) and their length varies based on the length of the joints. The positions and number of the shims are predetermined to give a desired non-persistent joint. Through these slits, greased metallic shims are inserted through the thickness of the mold before pouring the gypsum. The mold with the fresh gypsum is vibrated and then stored at room temperature for 8 h afterward. The specimens un-molded and the metallic shims pulled out of the specimens; the grease on the shims prevents adhesion with the gypsum and facilitates the removal of the shims. As the gypsum seated and hardened, each shim leaves in the specimen an open joint through the thickness and perpendicular to the front and back of the specimen. Immediately after removing the shims, the front and back faces of the specimens are polished and the specimen is stored in laboratory for 4 days. At the end of the curing process, the specimens are tested. It does not appear that the pull out of the shims produces any damage through the joints. The aperture of joints is 0.5 mm, therefore the joint surface has not any effect on the failure mechanism.

The coplanar rock bridges have various configurations respect to shear loading direction and have occupied 45 cm^2 , 90 cm^2 of the total shear surface (225 cm^2) respectively. The geometry and dimensions of non-persistent joints has shown in Figure 4 and Figure 5.

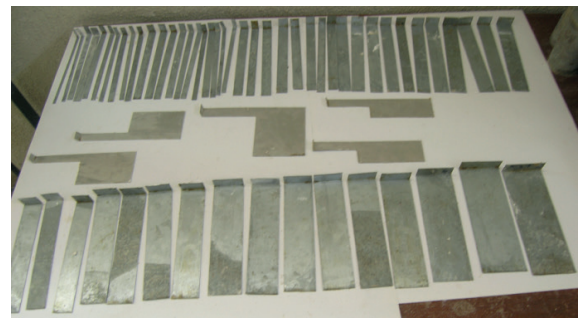
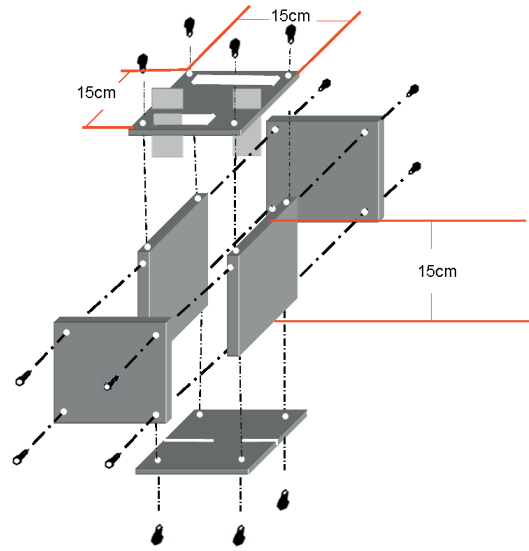


Fig. 3 Model used for the fabrication of the gypsum specimens

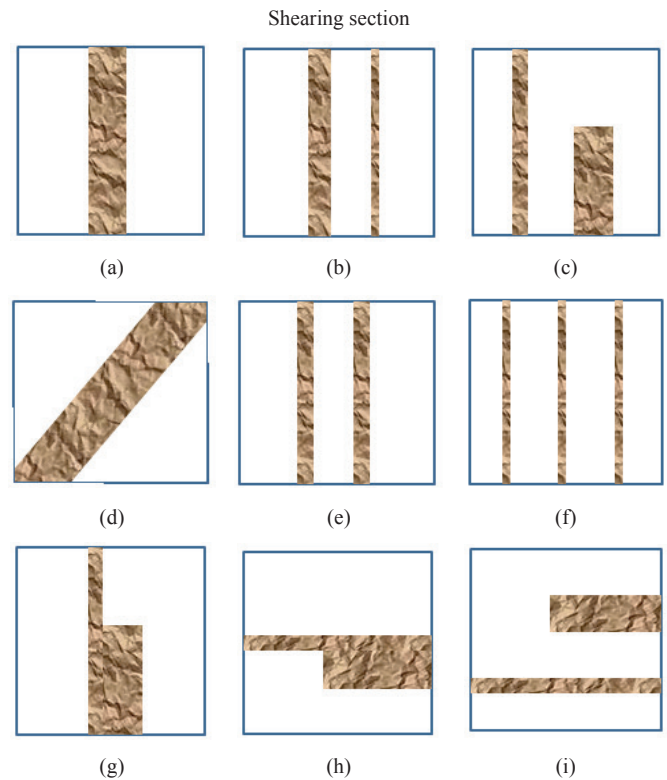


Fig. 4 The geometrical specifications of the various rock bridges; rock bridge area= 45 cm^2 .

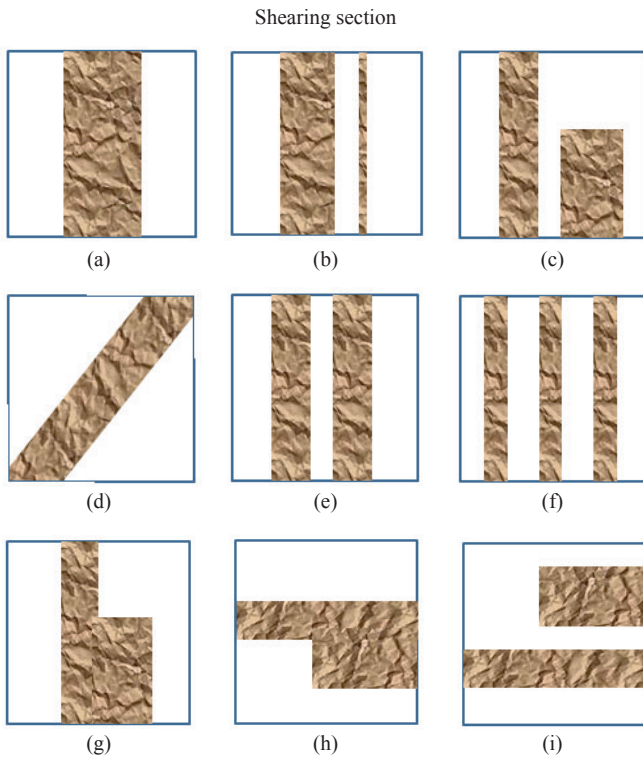


Fig. 5 The geometrical specifications of the various rock bridges; rock bridge area=90cm².

Based on the change in area of the rock-bridges, it is possible to define the Joint Coefficient, JC, as the ratio of rock bridge surface to the joint surface that is in front of the rock-bridge. Table 1 shows the amount of JC. In order to study the complete failure behaviour of rock bridges, from each model with special geometry, two similar blocks were prepared and were tested under normal stresses (σ_n) of 1 MPa. If the results from two identical tests show significant differences, a third specimen was prepared and tested.

Table 1 The amounts of the Joint Coefficients (JC) for various configurations

Rock bridge geometry	a	b	c	d	e	f	g	h	i
Rock bridge surface (cm ²)	45	45	45	45	45	45	45	45	45
Joint surface (cm ²)	180	180	160	200	180	180	180	60	60
JC	0.25	0.25	0.28	0.225	0.25	0.25	0.25	0.75	0.75
Rock bridge surface (cm ²)	90	90	90	90	90	90	90	90	90
Joint surface (cm ²)	135	135	105	155	135	135	135	45	45
JC	0.67	0.67	0.85	0.58	0.67	0.67	0.67	2	2

2.3 Testing program

A total of 18 direct shear tests have been performed on specimens with discontinuous joints. All tests are displacement-controlled. The tests were performed in such a way that the normal load, 1 MPa, was applied to the sample and then shear load was adopted. Readings of shear loads, as well as the shear displacements are taken by a data acquisition system. Loading is carried out at a rate of the 0.002 mm/s. The failure pattern was measured/observed after the test was completed. The shearing process of a discontinuous joint constellation begins, as one would expect, with the formation of new fractures which eventually transect the material bridges and lead to a through-going discontinuity.

3 Observation

By observing the failure surface after the tests, it is possible to investigate the effect of bridge configurations (or JC) on the failure mechanism of specimens. Figure 6 and 7 shows the tested models with rock bridge area of 45 cm² and 90 cm², respectively. The crack pattern is always a combination of only two types of cracks: wing cracks and shear cracks. Wing cracks start at the tip of the joints and propagate in a curvilinear path as the load increases. Wing cracks are tensile cracks and they grow in a stable manner, since an increase in load is necessary to lengthen the cracks. Shear cracks also initiate at tip of the joints and propagate in a stable manner.

3.1 The Failure pattern in rock bridges

Type I: The oval mode coalescence with two wing cracks

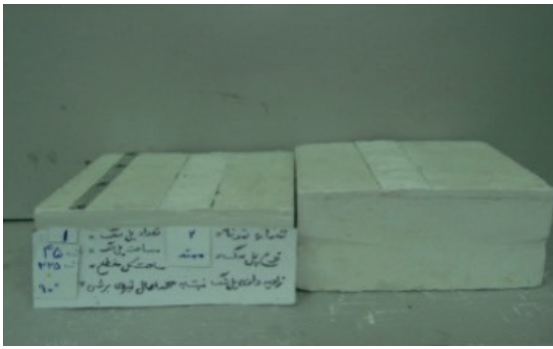
The oval mode coalescence, as defined in Fig. 6a, b, d, e, f and g, occurs when $JC \leq 0.25$. The wing cracks were initiated and propagated in curvilinear path that eventually aligned with the shear loading direction.

The wing cracks propagate in a stable manner; and the external load needs to be increased for the cracks to propagate further. Each wing crack was initiated at the tip of the one joint and finally coalesced with the tip of the other joint.

This coalescence left an oval core of intact material completely separated from the sample. The surface of failure is tensile because no crushed or pulverized materials and no evidence of shear movement were noticed. The wing cracks surfaces also had the same characteristics of tension surface.

Type II: Coalescence with mixed crack (shear/tensile)

This coalescence, as defined in Fig. 6c and Fig. 7d occurred when $0.25 < JC \leq 0.58$. At first the wing cracks were initiated at the tip of the joints and propagated stably. Wing cracks connect to each other by a shear crack. Examining the failure surface in near the joint tips, it was noticed that there was smooth and clean with no crushed or pulverized material and no evidence of shear displacement. These surface characteristics indicated that tensile stresses were responsible for the initiation and propagation of the wing cracks. Also the characteristics of the failure surface in the middle region were investigated.



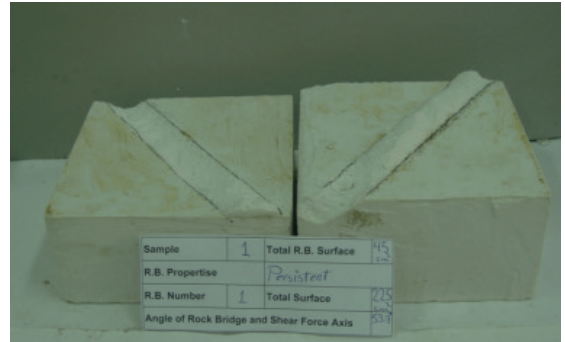
(a)



(b)



(c)



(d)



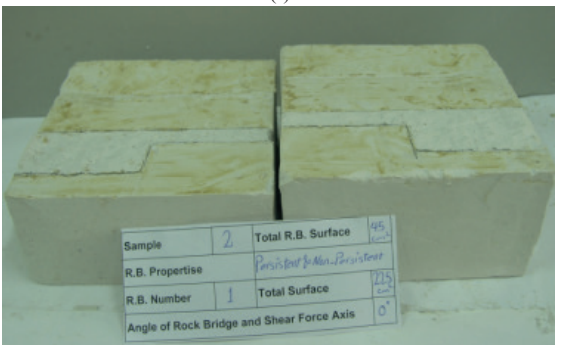
(e)



(f)



(g)

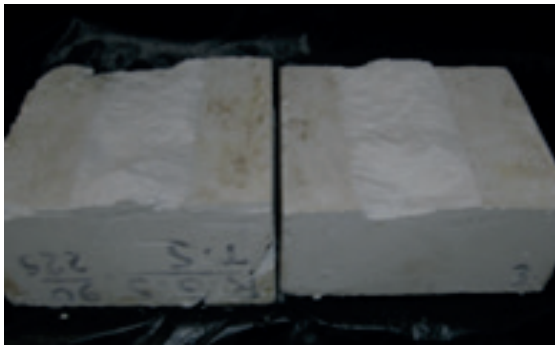


(h)



(i)

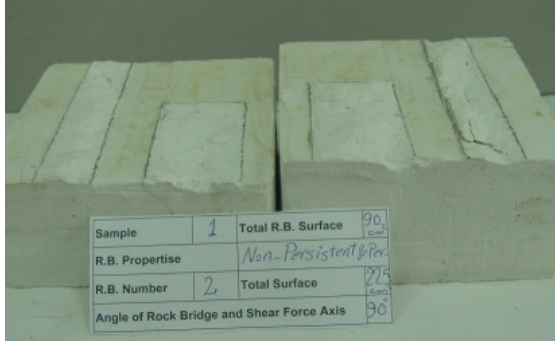
Fig. 6 Failure pattern in rock bridge with area of 45 cm².



(a)



(b)



(c)



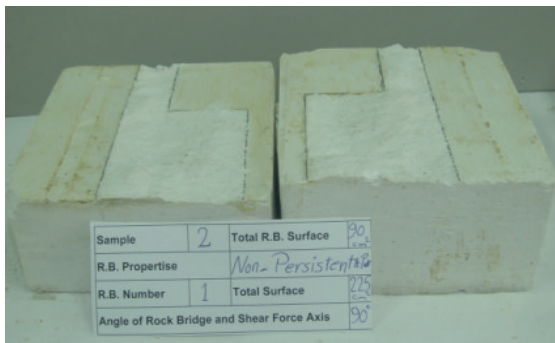
(d)



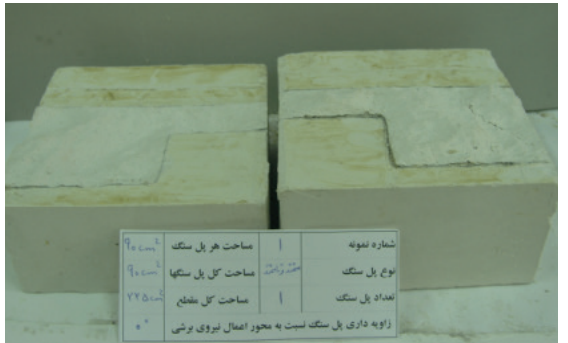
(e)



(f)



(g)



(h)



(i)

Fig. 7 Failure pattern in rock bridge with area of 90 cm².

There was a significant amount of pulverized and crushed gypsum and traces of shear displacement, indicated that a shearing failure had taken place.

Type III-Coalescence with two shear cracks

Coalescence with shear cracks, as defined in Fig. 6 h, i and Fig. 7 a, b, c, e, f, g, h and i, occurs when $EJC > 0.58$. The mechanism of failure was characterized first by initiation of wing cracks followed by the initiation of secondary cracks at the tips of the joint segments. Then the two wing cracks were stopped while the two secondary cracks were propagated to meet each other at a point in the bridge area. The propagation and coalescence of the secondary cracks brought rock bridges to failure. The shear failure surface is in a wavy mode. Inspection of the surface of the cracks producing coalescence reveals the presence of many small kink steps, crushed gypsum and gypsum powder, which suggested coalescence through shearing.

4 Description of the failure modes

The failure mode correlates quite well with the continuity of the joints and rock bridges, which can be described by the “joint coefficient”.

Type I: The oval mode coalescence with two wing cracks

For the rock-bridges with the $JC \leq 0.25$ (Fig. 6a, b, d, e, f and g), there is very large extension of joint surface in front of the rock-bridge tips (Table 1) and distance between the tip of the joints is short. Therefore a very high stress concentration (tensile and shear) is established due to the interaction between the joint tips. The tensile strength of the material existing at the tip of the joints is less than the shear strength and tensile stress intensity at tips of the joints is strong enough to produce the small tensile cracks tending to split the rock bridge. Since, the tensile stress intensity is not enough to cause unstable crack growth therefore an increase in external load is necessary to elongate the existing tensile cracks. After the wing crack has grown enough, the contribution of the wing opening to the stress field redistribution becomes significant. In this time, the crack-generated tensile stress field and the effect of interaction between the crack tip and opposite joint tip (that are indeed situated very close to each other) is so strong that tend to unstable wing cracks growth connecting the joints. Since no new fracture produces in the midst zone, the coalescence left an oval core of intact material completely separated from the sample.

Type II: Coalescence with mixed crack (shear/tensile):

This coalescence occurs when $0.25 < JC \leq 0.58$ (Fig. 6c and Fig. 7d). According to the characteristic of the failure surface, it seems that at first high tensile stresses concentration reaches to tensile strength of material existing at the tips of the joints and wing cracks initiate. The tensile strength of material is less than its shear strength so before the shear stresses concentration could overcome to shear strength, the tensile stress concentration reach to critical value and wing cracks initiate at tips of the joints. Afterward the wing cracks stopped suggesting

that the tensile stresses were eliminated at the wing cracks. With increasing external loading, the shear stresses concentration at tips of the wing cracks reaches to critical value and the new-born shear cracks is created at tips of the wing cracks. These shear cracks propagate till bring the rock bridge to failure.

Type III: Coalescence with two shear cracks:

This coalescence occurs when $JC > 0.58$ (Fig. 6 h, i and Fig. 7 a, b, c, e, f, g). In this case the high stress concentration (tensile and shear stresses) is established at tips of the joints due to high external loading. At first, the tensile stresses reach to critical value (because the tensile strength of the material existing at the tip of the joints is less than its shear strength) and two wing cracks initiated at the tips of the joints. The tensile stresses was released due to wing cracks initiated at the tips of the joints so two wing cracks were stopped. With increasing in external loading, the tensile stress concentration at tips of the wing cracks reach to critical value again and tensile cracks can propagate for a short distance in a curvilinear path. Before the wing cracks could propagate further, the shear stress concentration leads to the secondary cracks initiation at the tips of the pre-existing joints. The external shear loading must be increased that cause the shear stresses concentration at tips of the shear cracks overcome to shear strength of material. This shear cracks propagate till the end of the test. The propagation and coalescence of the secondary cracks brought rock bridges to failure in a wavy mode.

5 Description of the shear stress versus shear displacement curves

5.1 The effect of rock bridge shape on the shear stress versus shear displacement curve

Fig. 8 a and b shows shear stress versus shear displacement curves for rock bridge area of 45 cm^2 and 90 cm^2 , respectively. The rock bridges have various configurations. The inclination of the curve, or shear stiffness of rock bridge, was decreased with increasing the JC (Fig 8a and b). For example sample d, which has lowest JC , i.e. 0.225 and 0.57 for rock bridge area of 45 cm^2 and 90 cm^2 , respectively, show lowest shear stiffness. But sample i which has highest JC (0.75 and 2 for rock bridge area of 45 cm^2 and 90 cm^2 , respectively) has highest shear stiffness. In fact the stress concentration a tip of the joint was decreased by decreasing the JC so interlocking force between the grains was increased. This leads to increasing in the shear stiffness of rock bridge.

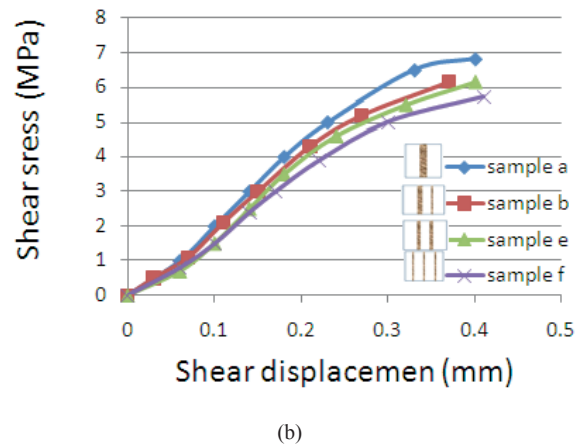
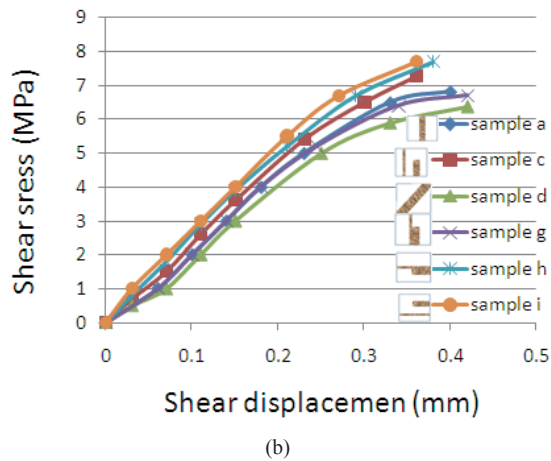
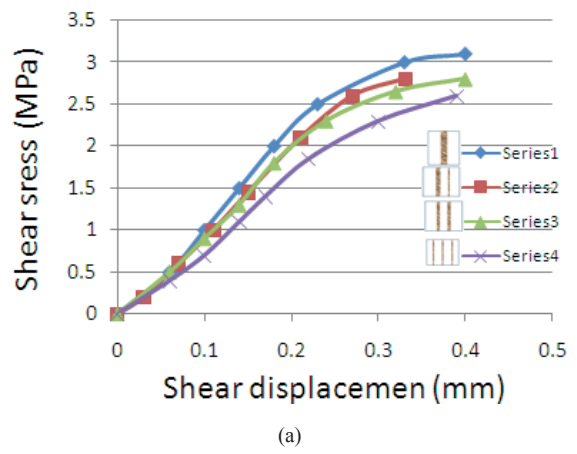
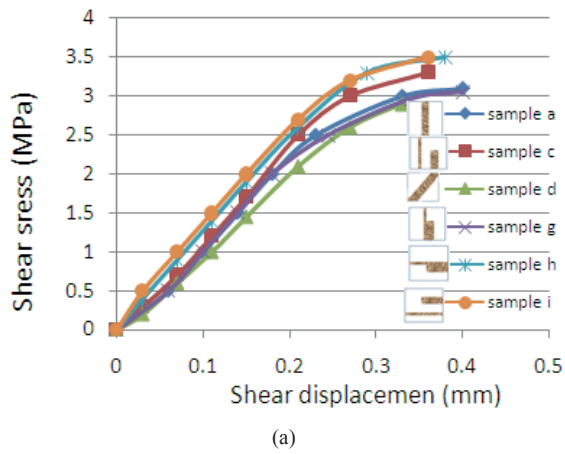


Fig. 8 Shear stress versus shear displacement curves for models with two rock bridge area; a) 45 cm², b) 90 cm².

Fig. 9 Shear stress versus shear displacement curves for the models with different rock bridge number; a) 45 cm², b) 90 cm².

5. 2 The effect of rock bridge number on the shear stress versus shear displacement curve

Fig. 9 a and b shows shear stress versus shear displacement curves for rock bridge area of 45 cm² and 90 cm², respectively. The rock bridges have various numbers, i.e. one rock bridge, two rock bridge and three rock bridge. The inclination of the curve, or shear stiffness of rock bridge, was decreased with increasing the rock bridge number (Fig 9a and b). For example sample a, which has one rock bridge, $JC = 0.25$ and 0.67 for rock bridge area of 45cm² and 90 cm², respectively, show highest shear stiffness. But samples f, which has three rock bridge, $JC = 0.25$ and 0.67 for rock bridge area of 45cm² and 90 cm², respectively, show lowest shear stiffness. In fact, in fixed area of rock bridge, the stress concentration at a tip of the joint was increased by increasing the rock bridge number so interlocking force between the grains was decreased. This leads to decreasing in the shear stiffness of rock bridge.

6 Shear strength of samples consisting various rock bridge

6.1 The effect of rock bridge shape on the shear strength of sliding surface

Fig. 10 a and b shows shear strength versus rock bridge configuration for rock bridge area of 45 cm² and 90 cm², respectively. Sample d has lowest shear strength. In this configuration, the lowest joint surface has occupied the shear surface therefore high stress concentration occurred at tip of the joint. This leads to decreasing in the shear strength.

Sample i has lowest shear strength. In this configuration, JC has maximum value, i.e. 0.75 and 2 for rock bridge area of 45cm² and 90 cm², respectively (Table 1). Whereas the lowest joint surface has occupied the shear surface therefore less stress concentration occurred at tip of the joint. This leads to increasing in shear strength.

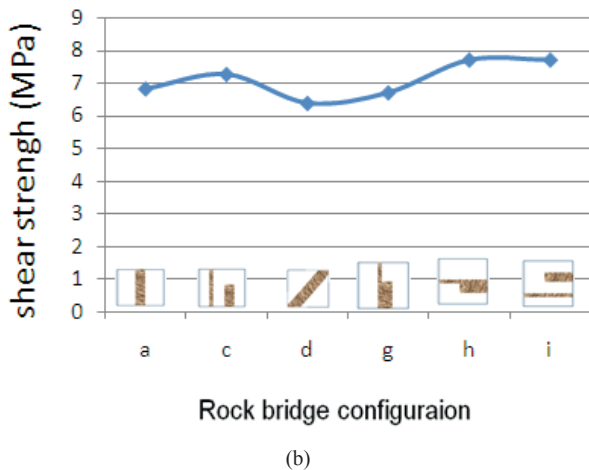
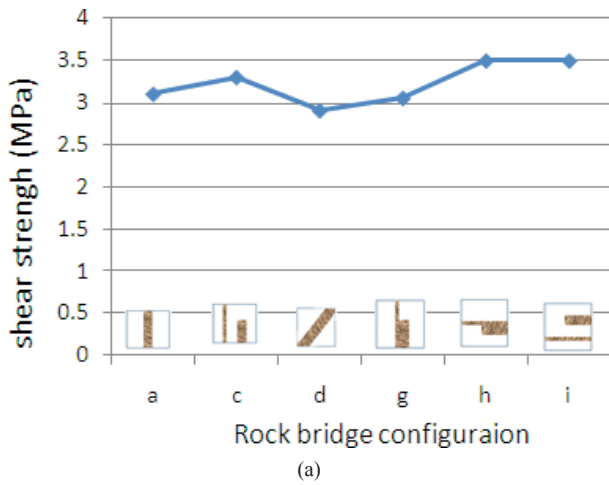


Fig. 10 Shear strength versus rock bridge configuration; rock bridge area is, a) 45 cm², b) 90 cm².

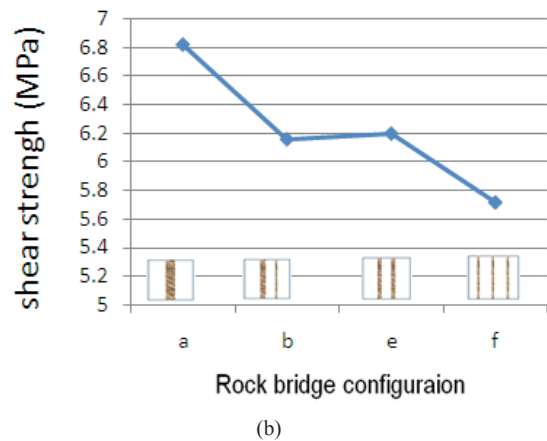
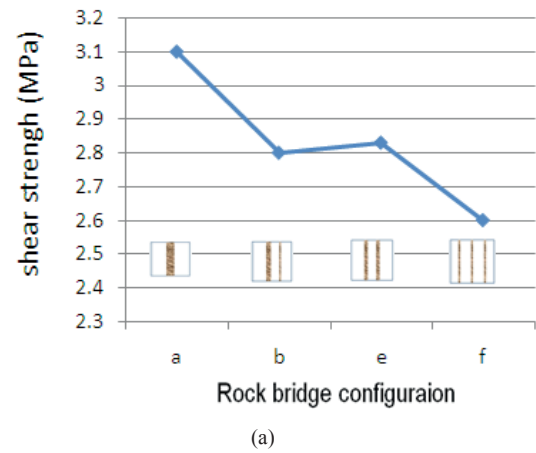


Fig. 11 Shear strength versus rock bridge number; rock bridge area is, a) 45 cm², b) 90 cm².

6.2 The effect of rock bridge number on the shear strength of sliding surface

Fig. 11 a and b shows shear strength versus rock bridge number for rock bridge area of 45 cm² and 90 cm², respectively. Sample a, which has one rock bridge, $JC = 0.25$ and 0.67 for rock bridge area of 45cm² and 90 cm², respectively, show highest shear strength. But samples f, which has three rock bridge, $JC = 0.25$ and 0.67 for rock bridge area of 45cm² and 90 cm², respectively, show lowest shear strength. In fact, in fixed area of rock bridge, the stress concentration a tip of the joint was increased by increasing the rock bridge number so interlocking force between the grains was decreased. This leads to decreasing in the shear strength of rock bridge.

7 Conclusions

The shear behaviour of rock-like specimens containing various configurations of rock bridges with different areas has been investigated through direct shear test. The results show that both of the failure pattern and failure mechanism are mostly influenced by JC . While both of the shear strength and shear stiffness are closely related to the ratio of rock bridge surface to joint surface and number of rock bridge. The following conclusions can be drawn from the experimental tests:

1. In the fixed area of the rock-bridge, with decreasing in Joint Coefficient, a very high stress concentration (tensile and shear stress) was established at tip of the joints due to the interaction between the joint tips.
2. The shear failure mode in the rock-bridge changes to the tensile failure mode by decreasing in the Joint Coefficient.
3. The shear strength is closely related to the rock bridge failure pattern and failure mechanism, so that in the fixed area of the rock-bridge, the rock-bridge resistance reduced with change in failure mode from shear to tensile.
4. For the fixed area of the rock bridge, the shear resistance along the failure surface increase with decreasing the number of rock bridge and increasing the JC .

References

- [1] Eberhardt, E., Stead, D., Coggan, J., Willenberg, H. "An integrated numerical analysis approach to the Randa rockslide." In: Proceedings of the First European Conference on Landslides, Prague, Czech Republic, June 24-26, 2002. pp. 355-332. 2002.
- [2] Hatzor, Y. H., Arzi, A. A., Zaslavsky, Y., Shapira, A. "Dynamic stability analysis of jointed rock slopes using the DDA method: King Herod's Palace, Masada, Israel." *International Journal of Rock Mechanics and Mining Sciences*. 41(5), pp. 813-832. 2004. DOI: [10.1016/j.ijrmms.2004.02.002](https://doi.org/10.1016/j.ijrmms.2004.02.002)
- [3] Vasarhelyi, B., Bobet, A. "Modeling of crack initiation, propagation and coalescence in uniaxial compression." *Rock Mechanics and Rock Engineering*. 33(2), pp. 119-139. 2000. DOI: [10.1007/s006030050038](https://doi.org/10.1007/s006030050038)
- [4] Wong, R. H. C., Chau, K. T. "Crack coalescence in a rock-like material containing two cracks." *International Journal of Rock Mechanics and Mining Sciences*. 35(2), pp. 147-164. 1998. DOI: [10.1016/S0148-9062\(97\)00303-3](https://doi.org/10.1016/S0148-9062(97)00303-3)
- [5] Shen, B. "The mechanics of fracture coalescence in compression experimental study and numerical simulation." *Engineering Fracture Mechanics*. 51(1), pp. 73-85. 1995. DOI: [10.1016/0013-7944\(94\)00201-R](https://doi.org/10.1016/0013-7944(94)00201-R)
- [6] Lajtai, E. Z. "Strength of discontinuous rock in direct shearing." *Geotechnique*. 19(2), pp. 218-233. 1969. DOI: [10.1680/geot.1969.19.2.218](https://doi.org/10.1680/geot.1969.19.2.218)
- [7] Li, C., Stephansson, O., Savilahti, T. "Behaviour of rock joints and rock bridges in shear testing." In: Rock joints: proceedings of the International Symposium on Rock Joints. Loen, Norway, June 4-6. 1990. (Ed. Nick Barton, Ove Stephansson) Rotterdam, Balkema Publishers, A.A. Taylor & Francis, The Netherlands, 1990, pp. 259-266.
- [8] Lajtai, E. Z. "Resistance of discontinuous rocks in direct shear" *Geotechnique*, 19, pp 218-233. see no. 6. ref.
- [9] Savilahti, T., Nordlund E. and Stephansson, O. "Shear box testing and modeling of joint bridge" In: In: Rock joints: proceedings of the International Symposium on Rock Joints. Loen, Norway, June 4-6. 1990. (Ed. Nick Barton, Ove Stephansson) Rotterdam, Balkema Publishers, A.A. Taylor & Francis. The Netherlands, 1990. pp. 295-300.
- [10] Wong, R. H. C., Leung, W. L., Wang, S. W. "Shear strength study on rock-like models containing arrayed open joints" In: *Rock mechanics in the national interest*. (Elsworth, D., Tinucci, J. P., Heasley, K. A. ed.) Swets & Zeitlinger Lisse. 2001.
- [11] Ghazvinian, A., Nikudel, M. R., Sarfarazi, V. "Effect of rock bridge continuity and area on shear behavior of joints" In: 11th Congress of the International Society for Rock Mechanics. Jul. 9-13, Lisbon, Portugal. pp 518-522.
- [12] Ghazvinian, A., Nikudel, M. R., Sarfarazi, V. "Determination of Sliding Path in Rock Slopes Containing Coplanar Non-Persistent Open Discontinuity." *World Applied Sciences Journal*. 3(4), pp 577-589. 2008.
- [13] Yang, S. Q., Dai, Y. H., Han, L. J., Jin, Z. Q. "Experimental study on mechanical behavior of brittle marble samples containing different flaws under uniaxial compression." *Engineering Fracture Mechanics*. 76(12), pp. 1833-1845. 2009. DOI: [10.1016/j.engfracmech.2009.04.005](https://doi.org/10.1016/j.engfracmech.2009.04.005)
- [14] Yang, S. Q., Jiang, Y. Z., Xu, W.Y., Chen, X. Q. "Experimental investigation on strength and failure behavior of pre-cracked marble under conventional triaxial compression." *International Journal of Solids and Structures*. 45(17), pp. 4796-4819. 2008. DOI: [10.1016/j.ijsostr.2008.04.023](https://doi.org/10.1016/j.ijsostr.2008.04.023)
- [15] Fujii, Y., Ishijim, Y. "Consideration of fracture growth from an inclined slit and inclined initial fracture at the surface of rock and mortar in compression." *International Journal of Rock Mechanics and Mining Sciences*. 41, pp. 1035-1041. 2004. URL: http://rock.eng.hokudai.ac.jp/fujii/publ/2004/Fujii_and_Ishijima_2004_Fracture_Growth_Author_Version.pdf
- [16] Wasantha, P. L. P., Ranjith, P. G., Shao, S. S. "Energy monitoring and analysis during deformation of bedded sandstone: use of acoustic emission." *Ultrasonics*. 54(1), pp. 217-226. 2014. DOI: [10.1016/j.ultras.2013.06.015](https://doi.org/10.1016/j.ultras.2013.06.015)
- [17] Zhang, X. P., Wong, L. N. Y. "Cracking process in rock-like material containing a single flaw under uniaxial compression: A numerical study based on parallel bonded-particle model approach." *Rock Mechanics and Rock Engineering*. 45(5), pp. 711-737. 2012. DOI: [10.1007/s00603-011-0176-z](https://doi.org/10.1007/s00603-011-0176-z)
- [18] Zhang, X. P., Wong, L. N. Y. "Crack initiation, propagation and coalescence in rock-like material containing two flaws: A numerical study based on bonded-particle model approach." *Rock Mechanics and Rock Engineering*, 46(5), pp. 1001-1021. 2013. DOI: [10.1007/s00603-012-0323-1](https://doi.org/10.1007/s00603-012-0323-1)
- [19] Bahaaddini, M., Sharrock, G., Hebblewhite, B. K. "Numerical investigation of the effect of joint geometrical parameters on the mechanical properties of a non-persistent jointed rock mass under uniaxial compression." *Computers and Geotechnics*. 49, pp. 206-225. 2013. DOI: [10.1016/j.compgeo.2012.10.012](https://doi.org/10.1016/j.compgeo.2012.10.012)
- [20] Sarfarazi, V., Ghazvinian, A., Schubert, W., Blumel, M., Nejadi, H. R. "Numerical Simulation of the Process of Fracture of Echelon Rock Joints." *Rock Mechanics and Rock Engineering*. 47(4), pp. 1355-1371. 2014. DOI: [10.1007/s00603-013-0450-3](https://doi.org/10.1007/s00603-013-0450-3)
- [21] Takeuchi, K. "Mixed-mode fracture initiation in granular brittle materials." M.S. Thesis, Massachusetts Institute of Technology, Cambridge. 1991.
- [22] Shen, B., Stephansson, O., Einstein, H. H., Ghahreman, B. "Coalescence of fractures under shear stress experiments." *Journal of geophysical Research: Solid Earth*. 100 (B4), pp. 5975-5990. 1995. DOI: [10.1029/95JB00040](https://doi.org/10.1029/95JB00040)
- [23] Bobet, A., Einstein, H. H. "Fracture coalescence in rock-type materials under uniaxial and biaxial compression." *International Journal of Rock Mechanics and Mining Research*. 35(7), pp. 863-888. 1998. DOI: [10.1016/S0148-9062\(98\)00005-9](https://doi.org/10.1016/S0148-9062(98)00005-9)
- [24] ASTM D2938. "Test method for unconfined compressive resistance of intact rock core specimens." ASTM. 1979.
- [25] ASTM C496. "Standard Test Method for Splitting Tensile Strength of Cylindrical Concrete Specimens." ASTM. 1971.